RSC Advances

ROYAL SOCIETY OF CHEMISTRY

www.rsc.org/advances

Green Synthesis of Reduced Graphene Oxide by a GRAS strain *Bacillus Subtilis* 168 with high biocompatibility to Zebrafish Embryos

Tingting Liu[1,2], Ling-Ling Jiang[3], Ming-Fang He[2], Zhengang Zhu[1,2], De-bin Wang[1,2], Tian-Shun Song[1,2,4]*, Wei-min Tan[1,5], Pingkai Ouyang[1,2,6] , Jingjing Xie[1,2,4,6]*

[1]State Key Laboratory of Materials-Oriented Chemical Engineering, Nanjing Tech University, Nanjing, PR China

[2]College of Life Science and Pharmaceutical Engineering, Nanjing Tech University, Nanjing, PR China

[3]College of Pharmaceutical Sciences, Nanjing Tech University, Nanjing, PR China

[4]Jiangsu Branch of China Academy of Science & Technology Development, Nanjing, PR China

[5]National Engineering Research Center for Coatings, CNOOC Changzhou Paint and Coatings Industry Research Institute, Changzhou, PR China

[6]National Engineering Technique Research Center for Biotechnology, Nanjing, PR China

*Correspondence and requests for materials should be addressed to J.X. (xiej@njtech.edu.cn) and T.S. (tshsong@njtech.edu.cn)

Present address: 30 South Puzhu Road, College of Biotechnology and pharmaceutical Engineering, Nanjing Tech University, Nanjing 211816, PR China. Tel.: +86 25 58139939

Abstract

Low toxicity and high biocompatibility graphene-based nanomaterials are in high demand within the biomedical fields. In this study, a highly biocompatible bacterially reduced graphene oxide (BRGO) was prepared by a "Generally Recognized As Safe" (GRAS) strain *Bacillus subtilis* 168 mediated with Vitamin K_3 (VK_3). The hypothesis of VK_3 mediating electron transfer between succinate:quinine oxidoreductase, from *B. subtilis* 168, and graphene oxide (GO) was proposed. BRGO was characterized by Raman spectroscopy, XPS and XRD and showed excellent properties. Furthermore, BRGO illustrates greater biocompatibility, with less toxicity, than GO and chemically reduced graphene oxide (CRGO) by zebrafish toxicity assessment, which demonstrates its great potential in various biomedical applications.

Keywords

Graphene, graphene oxide, *Bacillus subtilis*, Vitamin K_3, green synthesis, biocompatibility

Introduction

Graphene, consisting of a single-layer sp^2-hybridized carbon atom network, is a rapidly rising star in the field of material science[1]. It has attracted a significant amount of attention in recent decades, due to its exceptionally high crystal and electronic qualities, such as high surface-to-volume ratio[2], high electrical[3] and thermal conductivity[4], high mechanical strength[5], etc. Therefore, graphene and its derivatives are being studied in almost all the fields of science, medicine and engineering[6]. The application of graphene-based nanomaterials has been inclusively illustrated in medicine[7], electronics[8], energy storage[9, 10], electrochemical sensors[6] and so on. In particular, much attention has been paid to biomedical applications of graphene-based nanomaterials ranging from tissue engineering[11], bioimaging[12, 13], and drug delivery[14, 15] to biosensors[16] , over the past 5 years.

Differing from other applications, low toxicity and high biocompatibility are essential characteristics for biomedical applications, especially *in vivo*[17]. As the most promising method for large scale production of graphene, the process of chemical synthesizing graphene first oxidized the graphite to graphene oxide (GO)[18-20] and then reduced the GO to graphene, using strong chemical reducing agents in organic solvents[2, 21], such as hydrazine and sodium borohydride. Unfortunately, these strong chemical reducing agents and solvents usually are highly corrosive and toxic. For example, acute exposure to hydrazine can damage the human liver, kidneys, and central nervous system[22]. Therefore, the development of more biocompatible and eco-friendly approaches to GO reduction has been attempted. Several biological molecules have been used as

reducing agents, such as sodium citrate[23], vitamin C[24], reducing sugars[25] and microorganisms[26].

Among all these greener processes, bacterial reduction of GO has drawn a lot of attention. Since Salas first reported the production of graphene by reduction of GO *via Shewanella* respiration[26], many other microbial species, including *Escherichia fergusoni*[27], *Extremophiles bacteria*[28], *Pseudomonas aeruginosa*[29], *Gluconacetobacter xylinus*[30], *Bacillus marisflavi*[31] and *Shewanella oneidensis* MR-1[32], have successfully demonstrated their ability to reduce GO to graphene by themselves or with redox mediators. Recently two groups, independently, reported methods for the preparation of nitrogen (N) and sulfur (S)-doped graphenes, through bacterial treatment of GO[33,34]. All these bacterial reducing processes of GO were under mild and safe conditions and some bacterially reduced graphene oxide (BRGO) products showed good biocompatibility and potential in biomedical applications.

Bacillus subtilis is an important variety of industrial microorganism, which has a long application history in fermenting food [35] and is used mainly for the production of all kinds of industrial enzymes. *B. subtilis* has been used as a probiotic supplement and is known to be a "Generally recognized as safe" (GRAS) strain (Title 21 of the Code of Federal Regulations [21 CFR] and FDA Office of Premarket Approval list of microorganisms). Therefore in the present study, we report a method to reduce GO utilizing *B. subtilis* 168 as the reducing agent, in the presence of Vitamin K_3 (VK_3) acting as the redox mediator. Compared with previously reported microorganisms for GO reduction, *B. subtilis* is safer and can decrease the risks of introduction of toxic

metabolites in biomedical applications. The composition and structure characteristics of BRGO and GO were determined by Raman spectroscopy, Scanning electron microscopy (SEM), Transmission electron microscope (TEM)，X-ray photoelectron spectroscopy (XPS) and X-ray diffraction (XRD). The hypothesis of VK_3 mediating electron transfer between succinate:quinine oxidoreductase (SQR) from *B. subtilis* 168 and GO is proposed. Furthermore, the toxicity and biocompatibility of BRGO were evaluated by the *in vivo* toxicity assessment including hatching rate, viability, heart rate and body length using a zebrafish model. BRGO showed lower toxicity and higher biocompatibility when compared to GO and chemically reduced graphene oxide (CRGO), which illustrates BRGO's prospects in biomedical applications such as drug delivery, tissue engineering and so on.

Materials and Methods

Reagents, chemicals and strains

GO was purchased from Nanjing XFNANO Materials Tech Co., Ltd. VK_3 was purchased from Sigma-Aldrich (USA). 2-*n*-Heptyl-4-hydroxyquinoline-*N*-oxide (HQNO) was purchased from Cayman Chemical Company (USA). All other chemicals used were reagent grade or better. All aqueous solutions were dissolved with ultrapure water, which was prepared by an EPED-superpure water system (EPED-20TS, Shanghai Precision Instrument Co., LTD). All of the M9 medium, LB medium and GO were dissolved with ultrapure water, but VK_3 was dissolved with ethanol absolute. *B. subtilis* 168 (ATCC23857) was purchased from ATCC (USA).

Bacterial reduction of GO

B. subtilis 168 was grown in LB medium, at 37 ℃for 12 h, with shaking at 200 r/min. The bacterium was harvested by centrifugation (10,000g, 5 min) and washed thrice in sterile M9 medium (containing $Na_2HPO_4•7H_2O$, 12.8 gL^{-1}; K_2HPO_4, 3 gL^{-1}; NaCl, 0.5 gL^{-1}; NH_4Cl, 1 gL^{-1}; $MgSO_4$, 0.24 gL^{-1}; $CaCl_2$, 0.011 gL^{-1}; glucose, 4 gL^{-1}, pH 7.0). The resulting cell pellets were suspended in M9 medium. Final concentration of the cell resuspension solution was approximately $0.5*10^9$ cells/mL. The experimental systems were carried out in 25 mL serum bottles containing 10 mL of cell resuspension solution, 10μg VK_3 and 5 mg GO. Samples were periodically taken and analyzed spectrometrically, as described below. Control experiments, using solely *B. subtilis 168* and solely VK_3, were also performed. The reactions operated at 25 ± 2°C.

Succinate:quinine oxidoreductase (SQR) inhibition assay

In order to understand the mechanism of the VK_3 mediated *B. subtilis* reduction of GO, an SQR inhibition assay was carried out. The assay was performed similarly to the bacterial reduction assay of GO, **but varied the concentration of SQR inhibitor present in the system.** In each system, there is 10 mL of cell resuspension (approximately $0.2*10^9$ cells/mL), 10μg VK_3, 5 mg GO and various amounts of HQNO, which is 0 μmol/L, 10 μmol/L, 50 μmol/L and 100 μmol/L, respectively. The corrected OD_{600} absorbance values of each system were analyzed over time.

Analytical methods

GO reduction was monitored by a Multimode Microplate Reader (Molecular Devices SpectraMax Paradigm, USA), which detected the increase of OD_{600} after correcting for bacterial cells. The Raman spectra of pure carbon-based materials were measured

using a LabRam HR Evolution Raman Spectrometer (Jobin-Yvon Horiba Scientific, France) with a Confocal Microscope at room temperature. SEM images were obtained by a Quanta200 field emission transmission electron microscope (Philips，Japan). TEM images were taken with a JEM-200CX microscope (JEOL, Japan). The X-ray diffractometer (Smartlab, Japan), equipped with Cu Ka radiation (λ=0.1541 nm) over the 2θ range of 5-90°, was used to characterize the X-ray diffraction (XRD) of the samples. X-ray photoelectron spectra (XPS) were performed on a PHI 5000 VersaProbe Spectrometer (UlVAC-PHI, Japan).

Zebrafish housing and embryo collection

Wild-type zebrafish (*Danio rerio*; Tubingen line) were obtained from the Model Animal Research Center of Nanjing University. As previously described[57], adult zebrafish, less than 1-year-old, were maintained at 28.5 ℃ and a pH of 7±0.2 using a 14:10 h light/dark photoperiod. They were fed with live brine shrimp once daily and dry shrimp flakes twice a day[58]. Embryos were produced by pair-wise mating and raised at 28.5 ℃ in embryo medium (0.2 g/L of Instant Ocean® Salt in distilled water with 0.01% methylene blue). The zebrafish studies were approved by the Institutional Animal Care and Use Committee (IACUC) at Nanjing Tech University. All zebrafish studies and were carried out strict accordance with the recommendations in the "Guide for the Care and Use of Laboratory Animals" of the Jiangsu Institutes of Health (http://www.jsfzb.gov.cn/art/2009/9/11/art_461_16911.html).

Embryo toxicity test

Healthy embryos at 2 hours post fertilization (hpf) were selected and arrayed in a

48-well plate with 10 embryos per well. Embryos were then exposed to GO, CRGO, and BRGO each at 4 concentrations (0, 20, 50, 100, and 200 mg/L) dispersed in embryo medium. Three replicates were used for each concentration. All 48-well plates were kept at 28.5 ℃ with a 14:10 light-dark cycle.

The development of zebrafish embryos and larvae was observed under a dissecting microscope (Nikon, SMZ745T). The toxicological endpoint was at 72 hpf, including hatching rate, viability, heart rate, length of larvae and malformations. For mortality, death was defined as absence of heartbeat for larvae. The heart beat was observed clearly and recorded by an experimenter with a stopwatch. Larval length was measured using the microscope ruler.

Statistics

All biological experiments were repeated at least three times. Values were given as mean ± S.E.M. Data were analyzed using GraphPad Prism 5.0 software. Statistical significance was assessed by one-way ANOVA, and *P* values less than 0.05 were considered significant.

Results and discussion

Bacterial reduction of GO

Four formulations ((I) blank control (M9 medium), (II) redox mediator (VK_3), (III) *B. subtilis* 168 (B) and (IV) *B. subtilis* 168 with redox mediator ($B+VK_3$) were added to the suspension of GO (0.5 mg/ml) and incubated in the incubator at 25 ℃ for 24 hours under anaerobic conditions. As shown in Fig. 1, at start point, all 4 groups were yellowish brown, which was the color of the GO solution. In as fast as 0.5 hour, the

reduction of GO was observed by the change of the solution color from yellowish brown to black precipitate in bottle (IV), which contained both *B. subtilis* 168 as reducing agent and VK_3 as redox mediator. This color change can be attributed to the distinct structural and physicochemical properties between GO and BRGO. GO has numerous hydrophilic functional groups, which gives it good solubility, while BRGO has mostly hydrophobic groups which, in solution cause the formation of a black precipitate. In the control groups, there is no evident color change in either the only-bacterially-treated or the only-redox-mediator-treated GO in M9 solution.

In order to quantitatively analyze the reduction of GO, the corrected OD_{600} absorbance values of the samples were monitored[36]. As shown in Fig. 2a, there was an obvious difference between GO treated with both *B. subtilis* 168 and VK_3 (B+VK_3) and the two controls (B and VK_3) in the first 0.5 hour of reaction. For the controls, the corrected OD_{600} was 0.263(B) and 0.195(VK_3), respectively, while the corrected OD_{600} of reduced GO (B+VK_3) was 0.898. Afterwards, there was almost no increase of the corrected OD_{600} for the controls, while that for BRGO (B+VK_3) rose rapidly. Up to 10 hours, the corrected OD_{600} value (B+VK_3) reached 2.09 and continued stable then, which implied that the reaction basically was over. The huge differences in the corrected OD_{600} values between BRGO (B+VK_3) and controls (B and VK_3) indicate that the synergistic effect of the redox mediator VK_3 and *B. subtilis* 168 is critical for GO reduction.

Reaction mechanism analysis

So far, many bacteria have been reported to reduce GO to graphene by electron

transfer directly or with exogeneous redox mediators[27-33]. For example, *Pseudomonas aeruginosa*[29] and sulfate-reducing bacteria[33] can reduce GO to graphene by direct electron transfer. *Shewanella* has been reported to reduce GO to graphene by direct electron transfer through cytochromes MtrA, MtrB, and MtrC/OmcA[26]. Nevertheless, quinone mediators can also promote *shewanella*'s GO reduction rate[32].

In our study, *B. subtilis* could only reduce GO to graphene with the presence of redox mediator VK_3. VK_3 (menadione), also known as "menaphthone" belongs to the quinone superfamily, which has both a reduced hydroquinone state and an oxidized quinine conformation. Quinones have been well studied as redox mediators, transfering electrons from bacteria to ferric compounds[37], heavy metals[38,39] and nitroaromatic compounds[40], etc. Particularly, *B. subtilis* contains a transmembrane succinate:menaquinone oxidoreductase (SQR) which can transfer electrons from intracellular succinate to extracellular menaquinone[41].

In order to further explore the mechanism of the bacterial reduction of GO by VK_3 mediated *B. subtilis*, a SQR inhibition assay was performed. It is reported that 2-*n*-Heptyl-4-hydroxyquinoline-*N*-oxide (HQNO) is a menaquinone antagonist, which is a well-known inhibitor of *B. subtilis* SQR. It reacts with SQR and prevents the menaquinone binding. But the binding affinity of HQNO is not as strong as menaquinone[42]. The corrected OD_{600} absorbance values of the BRGO reaction mixing (GO, *B. subtilis* 168 and VK_3) with various concentrations of HQNO over time were monitored to quantitatively analyze the effect of HQNO on the biological reduction of GO. As shown in Fig. 2b, due to the lower affinity to SQR than VK_3, when only 10

μmol/L of HQNO was present in the system, the bacterial reduction of GO suppressed only a little. As HQNO concentration increased to 100 μmol/L, the VK_3 mediated bacterial reduction of GO was suppressed approximately 20%. This result is a strong proof of the biological GO reduction mechanism in which VK_3 might mediate the electron transfer between the SQR of *B. subtilis* 168 and GO.

Therefore, a mechanism by which VK_3 facilitates the reduction of GO was proposed as follows (Fig. 3). Through a third class of SQR, *B. subtilis* first transfers electrons from succinate (with a midpoint potential, E_m, equal to +30 mV) to VK_3 (E_m=-75 mV)[43]. Then, the reducing form of VK_3 transfers electrons to GO and forms BRGO. The oxidized VK_3 goes back to the SQR to receive electrons again.

Raman spectral analysis

As one of the most powerful tools for analyzing carbon materials, Raman spectroscopy is always used to distinguish the character differences between GO and reduced GO, such as the number of layers[44,45], defects[46] and so on. The Raman spectrum of graphene oxide (Fig. 4) displays two main features: the G-peak which is generally located at ~1588 cm^{-1} accounts for the first order scattering of the E_{2g} phonon from sp^2 carbon atoms and the D-peak located at ~1353 cm^{-1} accounts for the breathing mode of the κ-point phonon from A_{1g} symmetry. After the reduction of the GO by *B. subtilis* 168 mediated with VK_3, we observed an apparent red shift of the G-peak. The G-peak was broadened and shifted to 1581 cm^{-1}. It is reported that the wavenumber of the G-peak correlates with the number of layers[44,45]; the G peak of single layer GO is located at 1588 cm^{-1}, while that of bacterially reduced GO is red

shifted 7 cm^{-1}, suggesting the formation of 2-6 layers of bacterially reduced GO. Moreover, the variation in relative intensity of the G-peak usually reveals changes in the electronic conjugation state, which suggests an alteration in the number of sp^2 domains[47]. In comparison to pure GO, the intensity ratio (I_D/I_G) improved from 0.92 to 1.01 after reduction by *B. subtilis* 168 and VK_3, indicating the introduction of sp^3 defects after functionalization. The 2D peaks of BRGO appear at around 2681 cm^{-1}, exhibiting a broader and up-shifted peak in the Raman spectra, indicating the formation of multi-layer graphene sheets. The results of our Raman spectroscopy analysis are in good agreement with the previous studies[48], which indicated the positive reduction effect by *B. subtilis* 168 and VK_3.

SEM and TEM analysis

Both SEM and TEM microscopes are important tools for the observation of microscopic structure. The SEM images(Fig.5a) and TEM images (Fig.5c) reveal that GO has a wavy, folded shape and exists in the form of thin layers. As shown in Fig. 5b, SEM images reveal that the BRGO uniformly consists of several layers stacked on top of one another like sheets of paper. The TEM images (Fig. 5d) of the BRGO look like a transparent silk veil with crumpled or wrinkled structure, which indicates that the graphene formation consists of only a few layers.

XPS analysis

XPS is a very sensitive qualitative analysis technique used to determine the kinetic energy and number of electrons emitted, yeilding clues about the graphene's composition and electronic state. Therefore, XPS was performed to determine the

surface elements of GO and BRGO. As shown in Fig. 6a, the C1s XPS spectra peaks for pristine GO centered at 284, 284.8, 286 and 287.2 eV, which were assigned to C-C/C=C, C-OH, C-O-C and HO-C=O, respectively[49]. The peak intensity of the C-C/C=C bond was less prominent when compared with that of the C-O, C=O and O-C=O bonds in GO, demonstrating that the carbon sheets contained many oxygen-containing groups within the GO. As shown in Fig. 6b, in addition to the four peaks for GO, there were 5 peaks for the BRGO, and the positions of the peaks shifted slightly. The C1s of C-C/C=C, C-OH, C-O-C, C=O and HO-C=O were located at 284, 284.8, 285.8, 286.7 and 287.2 eV. The new peak was assigned to C=O, may be due to the reduction of C-O-C and HO-C=O. More importantly, after bacterial reduction, the strongest signal came from the C-C/C=C bond and the C-O bond had obviously decreased in intensity, the results confirmed that most of the oxygen containing functional groups were removed and the substantial sp^2 carbon characteristics had been partially restored by the VK_3 mediated *B. subtilis* 168 reduction of GO.

XRD analysis

As an effective method for investigating the interlayer changes and the crystalline properties of the synthesized material, XRD was carried out to characterize the GO and BRGO. Pristine exfoliated GO exhibits a diffraction peak at $2\theta=9.68^{o}$ (Fig.7), corresponding to an interlayer spacing (d-spacing) of 0.92 nm, which means that GO has a large interlayer distance due to the interposition of oxygen-containing functional groups, such as hydroxyl, epoxy, and carboxyl groups, during the oxidation process[50]. After GO reduction by *B. subtilis* 168 together with VK_3, the XRD pattern appeared

as a broad peak, centered around at $2\theta=24.18^{o}$, with a decreasing interlayer spacing of 0.37 nm, indicating the removal of oxygen-containing groups and the formation of a fewer layered graphene[51].

Hatching rate, viability, heart rate and body length assessment

The zebrafish has high homology with the human genome and thus has been used extensively in the study of vertebrate genetics, developmental biology[52] and drug screening[53]. Recently, the zebrafish gained acceptance as an animal model for "predictive toxicology" at the Food and Drug Administration's (FDA) National Center for Toxicological Research (NCTR) (http://www.fda.gov/ForConsumers/ConsumerUpdates/ucm343940.htm). European legislation also considers the zebrafish embryo an alternative to animal experiments and consistent with the 3R approach that is, reduction, refinement and replacement of the mammalian models for toxicity screening[54]. The Zebrafish model has been extensively used for toxicity screens over a wide array of nanomaterials, including metal nanoparticles, carbon-based nanomaterials and polymers[55]. Therefore, hatching rate, viability, heart rate and body length assessment were used to evaluate the toxicity and biocompatibility of GO, CRGO and BRGO *in vivo,* via the zebrafish model.

Hatching is considered an important event within the course of embryogenesis and thus is a key endpoint for the embryo toxicity test. The hatching rates of the zebrafish embryos exposed to the GO, CRGO and BRGO are shown in Fig. 8a. Compared with the BRGO-treated group, the CRGO and GO-treated groups showed a significant dose-dependent decrease in hatching rate. The hatching rates for embryos

treated with CRGO and GO were 93%, 73%, 53%, 43% and 83%, 80%, 70%, 53% at 20, 50, 100, 200 mg/L, respectively. On the other hand, BRGO had no effect on the hatching. We also observed that all three nanomaterials did not cause any malformation during embryogenesis. Most of the embryos that failed to hatch were dead after exposure to the nanomaterials. Subsequently, a similar dose-response pattern was found in the viability assay (Fig. 8b).

Heart rate is an important indicator for cardiovascular toxicity. The heart rates of the zebrafish embryos were recorded at 72 hpf after exposure to the 3 nanomaterials at different concentrations. The results are shown in Fig. 8c. The heart rate of the embryos exposed to GO and CRGO at 72 hpf was decreased over the test range from 20-200 mg/L, though the significance was only obvious within the 200 mg/L CRGO treatment group. The BRGO had no effect on the heart rate at any of the tested concentrations.

Similar results were observed in the body length assessment (Fig. 8d). The body length of embryos exposed to GO and CRGO at 72 hpf was decreased from 20-200 mg/L, but significance was only obvious within the 200 mg/L CRGO treatment group. Again, BRGO had no effect on the body length at any of the tested concentrations.

The hatching of the embryos seemed to display the most sensitivity to graphene material exposure among all these toxicity tests. As shown in the image of zebrafish embryos exposed to different concentrations of GO, CRGO and BRGO (Fig.9), the differences in the effect of these three graphene materials on hatching rate (Table 1) might be due to CRGO and GO impairing the enzyme digestion of the chorion by the

embryos or the CRGO and the GO may have aggregated and adhered to the surface of the chorion of the embryos[55].

Different from previously reported bacteria, our reducing agent *B. subtilis* is a "GRAS" microorganism which does not produce toxins and other pernicious proteins[56]. Therefore, the synthesis of BRGO by VK_3 mediated *B. subtilis* is a safer, as well as a more reliable, cost-effective and eco-friendly process. According to our zebrafish toxicity assessments, BRGO showed more biocompatibility and less toxicity than either GO or CRGO, which illuminates, its potential in biomedical application.

Conclusions

Here we have provided a demonstration of an eco-friendly approach to the reduction of GO using a "GRAS" strain of *B. subtilis* 168 mediated by VK_3, which opens up the possibility of a green synthesis of graphene. The mechanism of reduction that is proposed is that GO might be reduced by the VK_3 mediated electron transfer via the SQR of *B. subtilis* 168. The bacterial reduction of GO has been confirmed by Raman spectroscopy, XPS and XRD. Moreover, the *in vivo* toxicity assessment, including hatching rate, viability, heart rate and body length using the zebrafish model, illustrated that BRGO has a lower toxicity and higher biocompatibility when compared to GO and CRGO. This work broadens our knowledge of the synthesis of graphene by bacteria, while providing a safe and biocompatible reductant for the green synthesis of nanomaterials.

Acknowledgements

This study was supported by the National Basic Research Program of China (973) (Grant No.: 2012CB721100, 2011CBA00806); the National Science Fund of China (Grant No.: 21306083, 21390201); the Fund from the State Key Laboratory of Materials-Oriented Chemical Engineering (ZK201312); Technology supporting program of Jiangsu Province (Grant No.: BE2014901) and the Priority Academic Program from Development of Jiangsu Higher Education Institutions.

Reference

1. A. K. Geim and K. S. Novoselov, *Nat Mater*, 2007, **6**, 183-191.
2. S. Stankovich, D. A. Dikin, G. H. Dommett, K. M. Kohlhaas, E. J. Zimney, E. A. Stach, R. D. Piner, S. T. Nguyen and R. S. Ruoff, *Nature*, 2006, **442**, 282-286.
3. K. S. Novoselov, A. K. Geim, S. V. Morozov, D. Jiang, Y. Zhang, S. V. Dubonos, I. V. Grigorieva and A. A. Firsov, *Science*, 2004, **306**, 666-669.
4. S. Chen, Q. Wu, C. Mishra, J. Kang, H. Zhang, K. Cho, W. Cai, A. A. Balandin and R. S. Ruoff, *Nat Mater*, **11**, 203-207.
5. C. Lee, X. Wei, J. W. Kysar and J. Hone, *Science*, 2008, **321**, 385-388.
6. A. T. Lawal, *Talanta*, 2015, **131**, 424-443.
7. S. Goenka, V. Sant and S. Sant, *J Control Release*, 2013, **173**, 75-88.
8. Y. Zhu, S. Murali, W. Cai, X. Li, J. W. Suk, J. R. Potts and R. S. Ruoff, *Adv Mater*, **22**, 3906-3924.
9. M. D. Stoller, S. J. Park, Y. W. Zhu, J. H. An and R. S. Ruoff, *Nano Letters*, 2008, **8**, 3498-3502.
10. S. Z. Zhu and T. Li, *Acs Nano*, 2014, **8**, 2864-2872.
11. G. Lalwani, A. M. Henslee, B. Farshid, L. Lin, F. K. Kasper, Y. X. Qin, A. G. Mikos and B. Sitharaman, *Biomacromolecules*, 2013, **14**, 900-909.
12. S. Kanakia, J. D. Toussaint, S. M. Chowdhury, G. Lalwani, T. Tembulkar, T. Button, K. R. Shroyer, W. Moore and B. Sitharaman, *Int J Nanomedicine*, 2013, **8**, 2821-2833.
13. G. Lalwani, X. Cai, L. Nie, L. V. Wang and B. Sitharaman, *Photoacoustics*, 2013, **1**, 62-67.
14. Z. Liu, J. T. Robinson, X. Sun and H. Dai, *J Am Chem Soc*, 2008, **130**, 10876-10877.
15. R. Tkacz, R. Oldenbourg, S. B. Mehta, M. Miansari, A. Verma and M. Majumder, *Chem Commun (Camb)*, 2014, **50**, 6668-6671.
16. R. S. Dey and C. R. Raj, *Journal of Physical Chemistry C*, 2010, **114**, 21427-21433.
17. M. A. Eckert, P. Q. Vu, K. Zhang, D. Kang, M. M. Ali, C. Xu and W. Zhao, *Theranostics*, 2013, **3**, 583-594.
18. K. Rajavel, C. R Minitha, K. S Ranjith and R. T Rajendra Kumar, *Recent patents on nanotechnology*, 2012, **6**, 99-104.

19. L. L. Abell, B. B. Levy, B. B. Brodie and F. E. Kendall, *Journal of Biological Chemistry*, 1952, **195**, 357-366.
20. G. B. Rybicki and D. G. Hummer, *Astronomy and Astrophysics*, 1991, **245**, 171-181.
21. H. J. Shin, K. K. Kim, A. Benayad, S. M. Yoon, H. K. Park, I. S. Jung, M. H. Jin, H. K. Jeong, J. M. Kim, J. Y. Choi and Y. H. Lee, *Advanced Functional Materials*, 2009, **19**, 1987-1992.
22. United States Environmental Protection Agency. Hydrazine Hazard Summary. 2000 (http://www.epa.gov/airtoxics/hlthef/hydrazin.html)
23. Z. Zhang, H. H. Chen, C. Y. Xing, M. Y. Guo, F. G. Xu, X. D. Wang, H. Gruber, B. L. Zhang and J. L. Tang, *Nano Research*, 2011, **4**, 599-611.
24. M. J. Fernandez-Merino, L. Guardia, J. I. Paredes, S. Villar-Rodil, P. Solis-Fernandez, A. Martinez-Alonso and J. M. D. Tascon, *Journal of Physical Chemistry C*, 2010, **114**, 6426-6432.
25. C. Z. Zhu, S. J. Guo, Y. X. Fang and S. J. Dong, *Acs Nano*, 2010, **4**, 2429-2437.
26. E. C. Salas, Z. Z. Sun, A. Luttge and J. M. Tour, *Acs Nano*, 2010, **4**, 4852-4856.
27. S. Gurunathan, J. W. Han, V. Eppakayala, M. Jeyaraj and J. H. Kim, *J Nanosci Nanotechnol*, 2013, **13**, 2091-2098.
28. S. Raveendran, N. Chauhan, Y. Nakajima, H. Toshiaki, S. Kurosu, Y. Tanizawa, R. Tero, Y. Yoshida, T. Hanajiri and T. Maekawa, *Particle & Particle Systems Characterization*, 2013, **30**, 573-578.
29. S. Gurunathan, J. W. Han, V. Eppakayala and J.-H. Kim, *Colloids and surfaces B: Biointerfaces*, 2013, **105**, 58-66.
30. A. G. Nandgaonkar, Q. Wang, K. Fu, W. E. Krause, Q. Wei, R. Gorga and L. A. Lucia, *Green Chemistry*, 2014, **16**, 3195.
31. S. Gurunathan, J. W. Han, V. Eppakayala and J.-H. Kim, *International journal of nanomedicine*, 2013, **8**, 1015.
32. G. Liu, X. Zhang, J. Zhou, A. Wang, J. Wang, R. Jin and H. Lv, *Bioresour Technol*, 2013, **149**, 503-508.
33. P. Guo, F. Xiao, Q. Liu, H. Liu, Y. Guo, J. R. Gong, S. Wang and Y. Liu, *Sci Rep*, 2013, **3**, 3499.
34. M. Fan, C. Zhu, Z. Q. Feng, J. Yang, L. Liu and D. Sun, *Nanoscale*, 2014, **6**, 4882-4888.
35 Y.Yuan, F.Feng, L.Chen,and K. Chen. *European Food Research and Technology*, 2013, 238, 285-293.
36. G. M. Wang, F. Qian, C. Saltikov, Y. Q. Jiao and Y. Li, *Nano Research*, 2011, **4**, 563-570.
37. T. Borch, W. P. Inskeep, J. A. Harwood and R. Gerlach, *Environmental Science & Technology*, 2005, **39**, 7126-7133.
38. S. Yamamura, M. Watanabe, M. Kanzaki, S. Soda and M. Ike, *Environmental Science & Technology*, 2008, **42**, 6154-6159.
39. B. H. Jeon, S. D. Kelly, K. M. Kemner, M. O. Barnett, W. D. Burgos, B. A. Dempsey and E. E. Roden, *Environmental Science & Technology*, 2004, **38**, 5649-5655.
40. R. P. Schwarzenbach, R. Stierli, K. Lanz and J. Zeyer, *Environmental Science & Technology*, 1990, **24**, 1566-1574.
41. L Hederstedt, *Biochimica et Biophysica Acta*, 2002, **1553**, 74-83.
42. I. A. Smirnova, A. A. Konstantinov and L. Hederstedt, *FEBS Letters*,1994,**359**,23-26
43. C. Hagerhall, *Biochim Biophys Acta*, 1997, **1320**, 107-141.

44. D. C. Wei, Y. Q. Liu, Y. Wang, H. L. Zhang, L. P. Huang and G. Yu, *Nano Letters*, 2009, **9**, 1752-1758.
45. D. Graf, F. Molitor, K. Ensslin, C. Stampfer, A. Jungen, C. Hierold and L. Wirtz, *Nano Letters*, 2007, **7**, 238-242.
46. A. Das, B. Chakraborty and A. K. Sood, *Bulletin of Materials Science*, 2008, **31**, 579-584.
47. S. Niyogi, E. Bekyarova, M. E. Itkis, H. Zhang, K. Shepperd, J. Hicks, M. Sprinkle, C. Berger, C. N. Lau, W. A. deHeer, E. H. Conrad and R. C. Haddon, *Nano Lett*, 2010, **10**, 4061-4066.
48. S. Gurunathan, J. W. Han, V. Eppakayala and J. H. Kim, *Colloids Surf B Biointerfaces*, 2013, **105**, 58-66.
49. S. Stankovich, D. A. Dikin, R. D. Piner, K. A. Kohlhaas, A. Kleinhammes, Y. Jia, Y. Wu, S. T. Nguyen and R. S. Ruoff, *Carbon*, 2007, **45**, 1558-1565.
50. D. R. Dreyer, S. Park, C. W. Bielawski and R. S. Ruoff, *Chemical Society Reviews*, 2010, **39**, 228-240.
51. I. K. Moon, J. Lee, R. S. Ruoff and H. Lee, *Nature Communications*, 2010, **1**.
52. A. F. Schier, *Nature*, 2013, **496**, 443-444.
53. A. J. Rennekamp and R. T. Peterson, *Current opinion in chemical biology*, 2014, **24C**, 58-70.
54. H. Sukardi, H. T. Chng, E. C. Chan, Z. Gong and S. H. Lam, *Expert opinion on drug metabolism & toxicology*, 2011, **7**, 579-589.
55. V. E. Fako and D. Y. Furgeson, *Advanced drug delivery reviews*, 2009, **61**, 478-486.
56. A. S. de Boer and B. Diderichsen, *Appl Microbiol Biotechnol*, 1991, **36**, 1-4.
57. M. F. He, X. P. Gao, S. C. Li, Z. H. He, N. Chen, Y. B. Wang and J. X. She, *European journal of pharmacology*, 2014, **740**, 240-247.
58. M. Westerfield, The University of Oregon Press, Eugene, OR, Editon edn., 2007.

Figure Captions

Fig.1 Time-course digital photographs of GO reduction with different reaction conditions: (I) blank control, (II) redox mediator (VK_3), (III) *B. subtilis* 168, (IV) *B. subtilis* 168 with redox mediator (VK_3)

Fig.2 Corrected OD_{600} values change over time: (a) Corrected OD_{600} values change over time on GO reduction with different reaction conditions (GO+VK_3 was shown in black squares, GO+B was shown in red dots, GO+B+VK_3 was shown in blue triangles) (b) Corrected OD_{600} values change of SQR inhibition assay (the concentration of HQNO, which was 0 μmol/L, 10 μmol/L, 50 μmol/L and 100 μmol/L, was shown in black squares, red dots, blue equilateral triangles and green inverted triangles, respectively.)

Fig.3 Electron transfer between *B. subtilis* 168 and GO mediated by VK3

Fig.4 Raman spectra with low (a) and high (b) resolution of GO and BRGO

Fig.5 SEM and TEM images of GO (a and c) and BRGO (b and d)

Fig.6 High-resolution XPS C1s spectra of (a) GO and (b) BRGO, and the survey XPS spectra of (c) BRGO and GO

Fig.7 XRD patterns on BRGO and GO

Fig.8 Toxicity assessment of three graphene materials. (a) hatching rate, (b) viability, (c) heart rate and (d) body length of zebrafish embryos exposed to GO, CRGO, and BRGO, at concentrations ranging from 20 to 200 mg/L. Each point represents a mean ±standard error of the mean (SEM) from a representative experiment. * $P < 0.05$, ** $P < 0.01$, and *** $P < 0.001$ in one-way ANOVA

analysis followed by the Dunnett multiple comparision test.

Fig.9 Effect of exposure to different concentrations (0, 20, 50,100, 200 mg/L) of (a) GO, (b) CRGO, (C) BRGO on the surface of the chorion of zebrafish embryos. Photos were taken at 24 hpf.

Table. 1. Hatching rate (%) of zebrafish embryos treated by GO, CRGO, and BRGO at different concentrations.

Concentration(mg/L)	0	20	50	100	200
GO	83	83	80	70	53
CRGO	93	93	73	53	43
BRGO	96	93	76	86	83

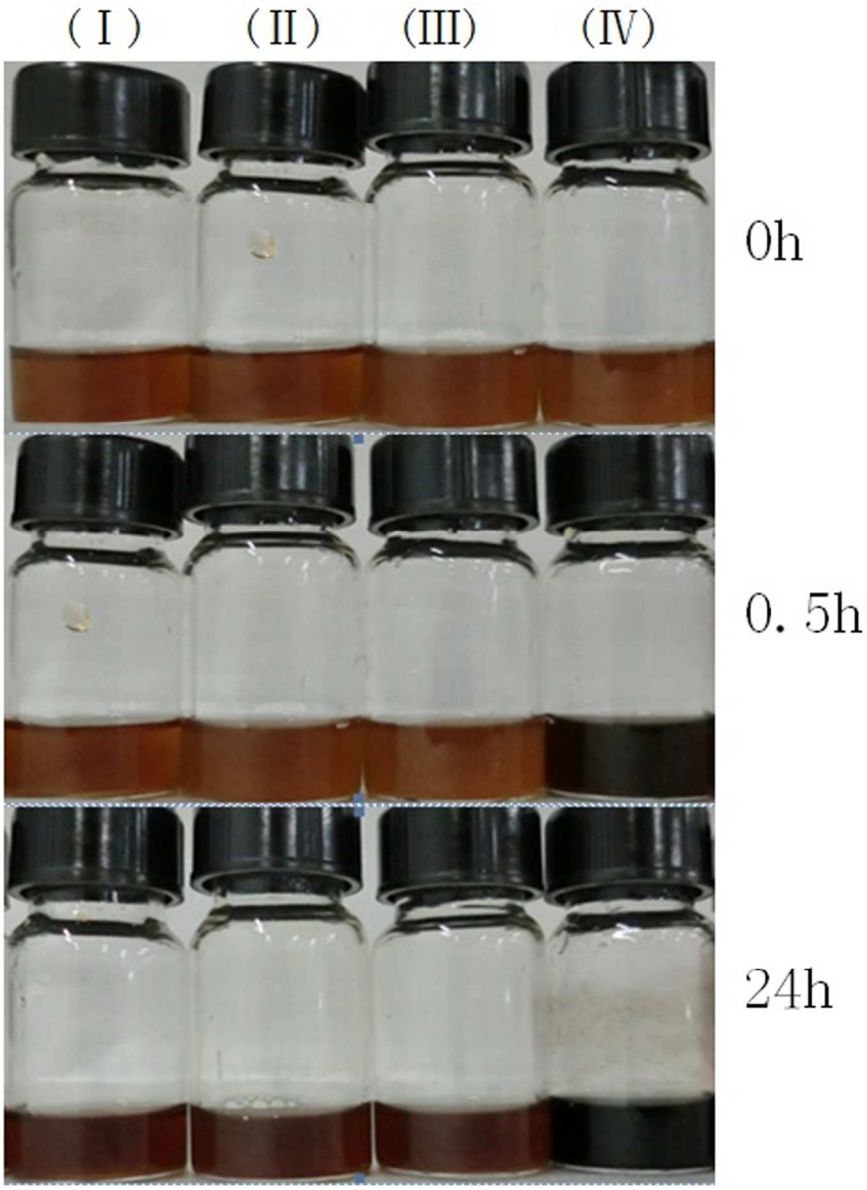

Time-course digital photographs of GO reduction with different reaction conditions: (I) blank control, (II) redox mediator (VK3), (III) B. subtilis 168, (IV) B. subtilis 168 with redox mediator (VK3)
111x148mm (300 x 300 DPI)

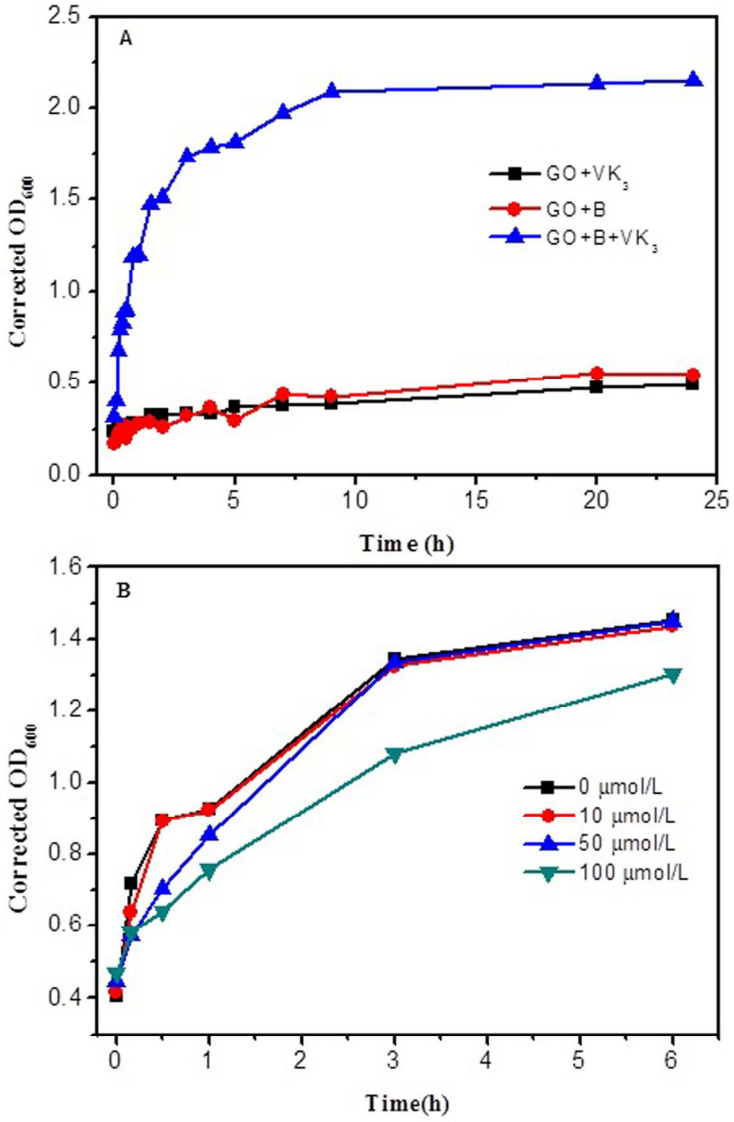

Corrected OD600 values change over time: (a) Corrected OD600 values change over time on GO reduction with different reaction conditions (GO+VK3 was shown in black squares, GO+B was shown in red dots, GO+B+VK3 was shown in blue triangles) (b) Corrected OD600 values change of SQR inhibition assay (the concentration of HQNO, which was 0 μmol/L, 10 μmol/L, 50 μmol/L and 100 μmol/L, was shown in black squares, red dots, blue equilateral triangles and green inverted triangles, respectively.)
109x144mm (300 x 300 DPI)

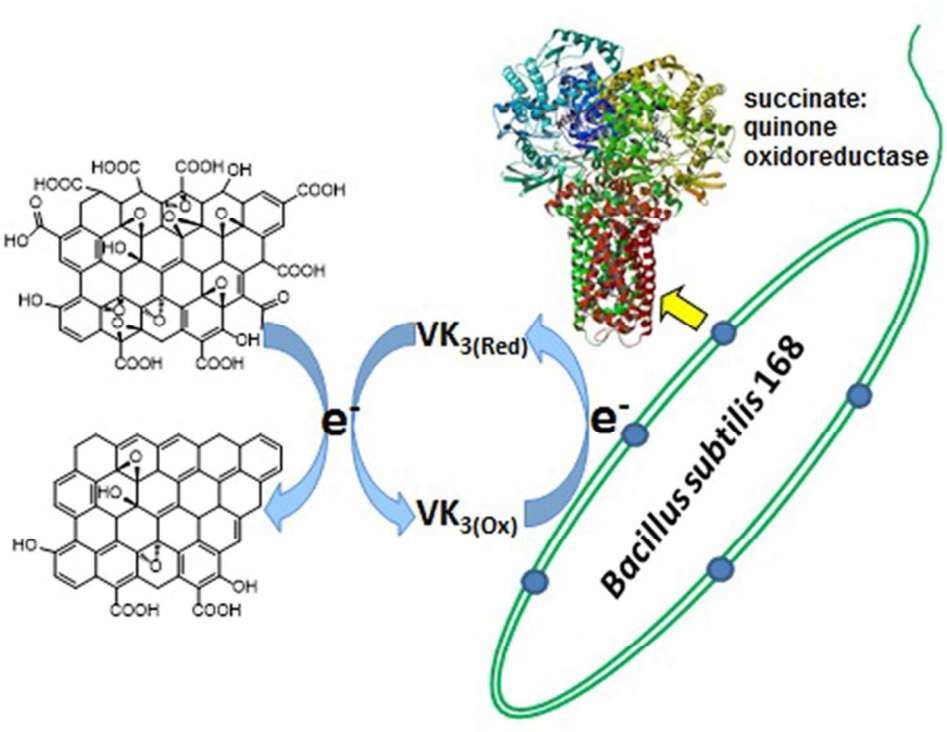

Electron transfer between B. subtilis 168 and GO mediated by VK3
62x46mm (300 x 300 DPI)

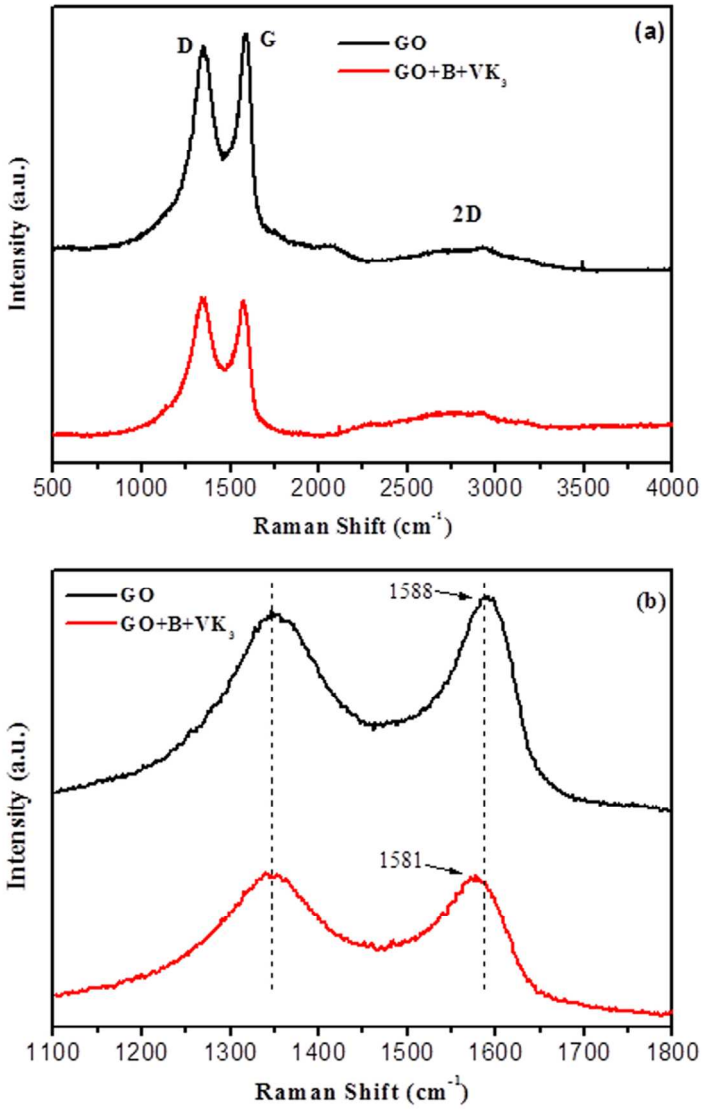

Raman spectra with low (a) and high (b) resolution of GO and BRGO
109x145mm (300 x 300 DPI)

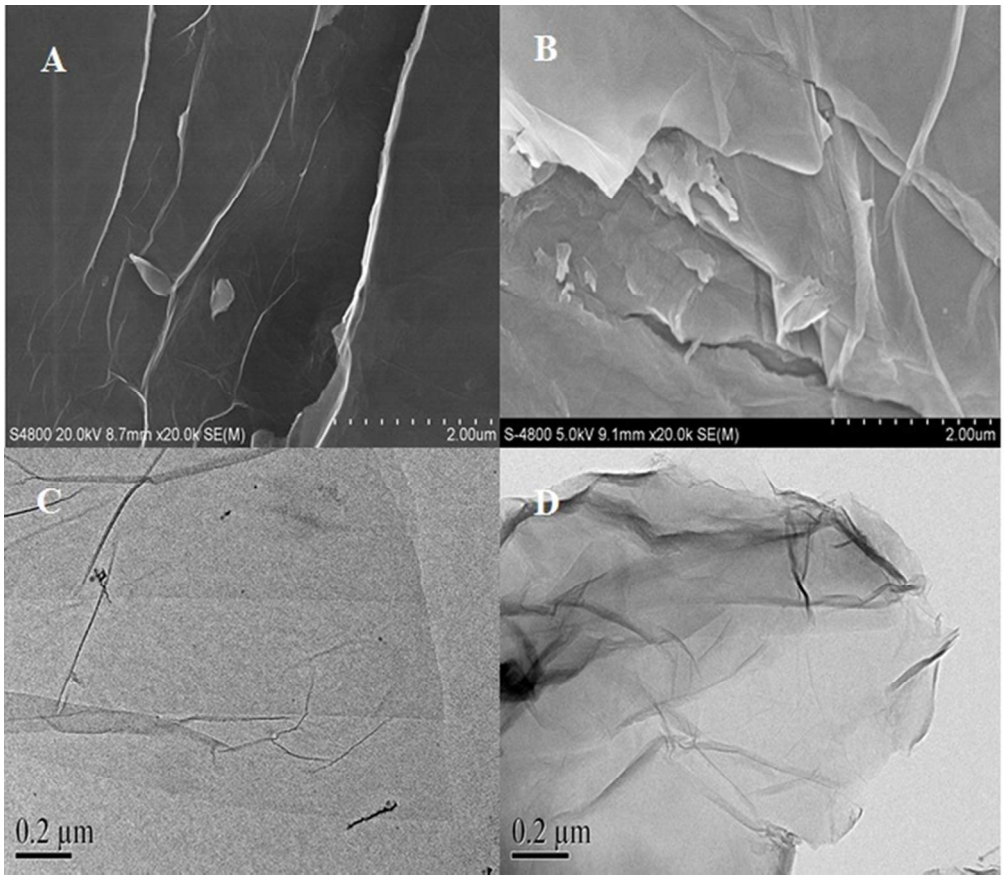

SEM and TEM images of GO (a and c) and BRGO (b and d)
72x62mm (300 x 300 DPI)

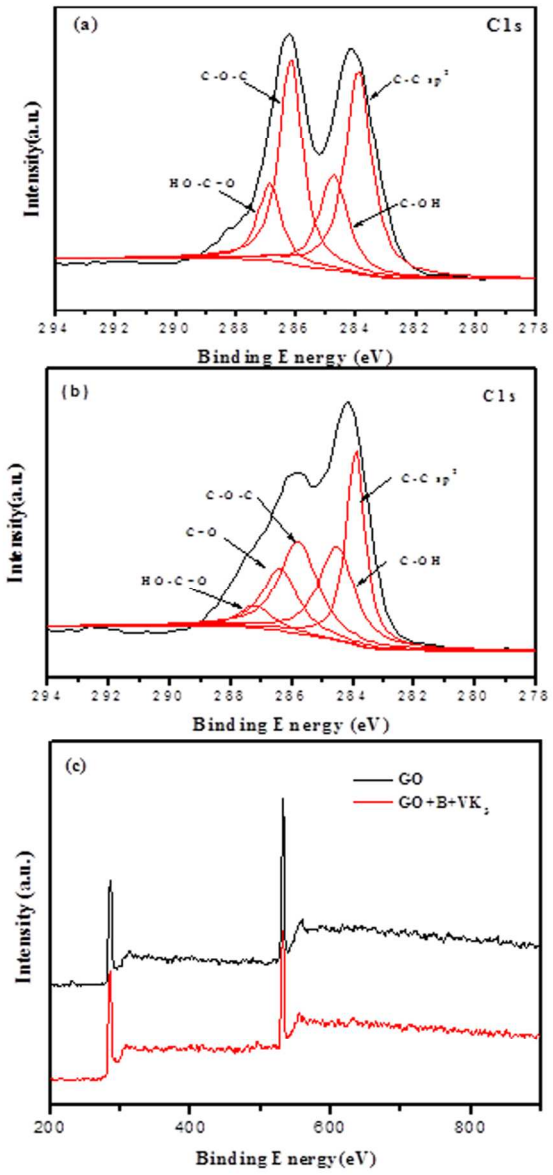

High-resolution XPS C1s spectra of (a) GO and (b) BRGO, and the survey XPS spectra of (c) BRGO and GO
140x238mm (300 x 300 DPI)

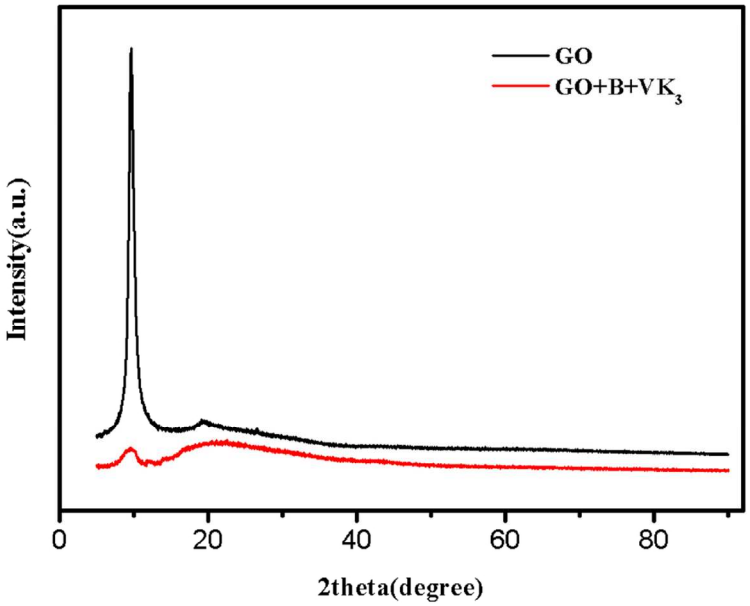

XRD patterns on BRGO and GO
58x40mm (600 x 600 DPI)

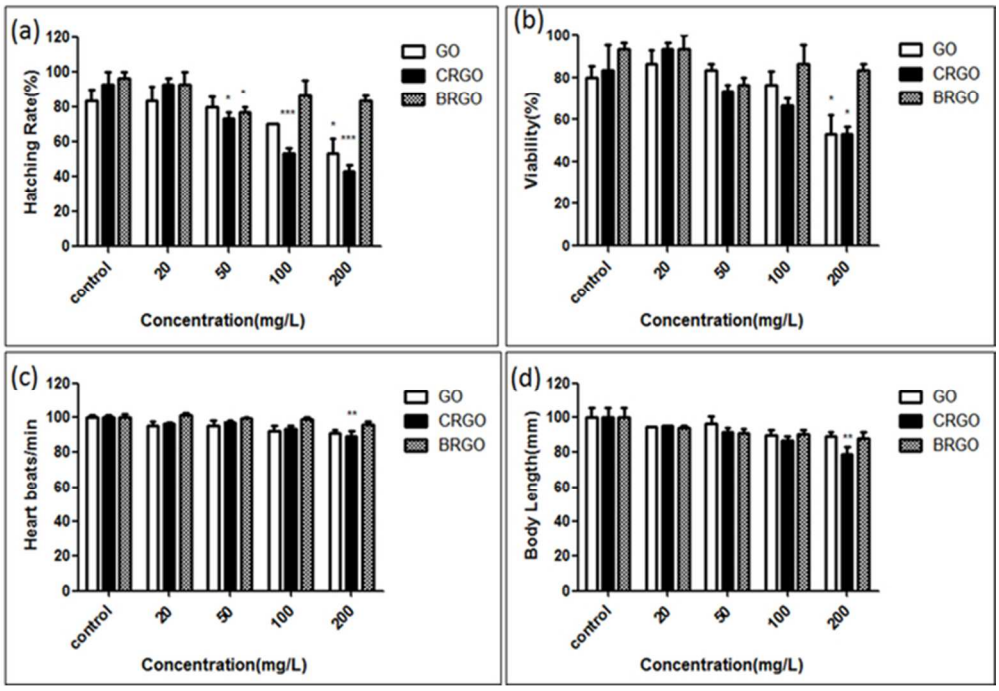

Toxicity assessment of three graphene materials. (a) hatching rate, (b) viability, (c) heart rate and (d) body length of zebrafish embryos exposed to GO, CRGO, and BRGO, at concentrations ranging from 20 to 200 mg/L. Each point represents a mean ±standard error of the mean (SEM) from a representative experiment. * $P < 0.05$, ** $P < 0.01$, and *** $P < 0.001$ in one-way ANOVA analysis followed by the Dunnett multiple comparision test.
57x39mm (300 x 300 DPI)

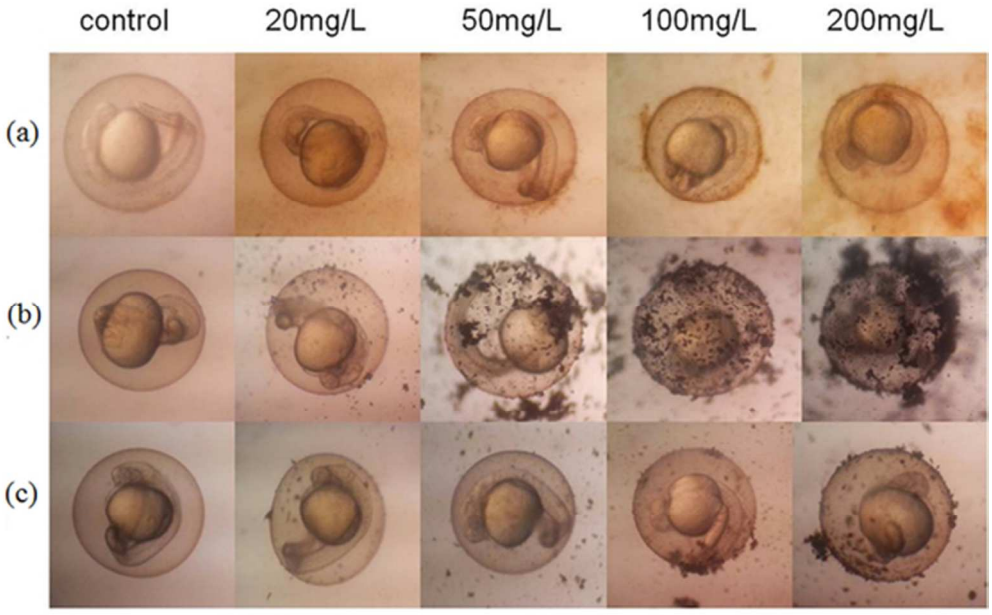

Effect of exposure to different concentrations (0, 20, 50,100, 200 mg/L) of (a) GO, (b) CRGO, (C) BRGO on the surface of the chorion of zebrafish embryos. Photos were taken at 24 hpf.
52x32mm (300 x 300 DPI)